



Published in final edited form as:

*Circulation*. 2003 May 6; 107(17): 2181–2184. doi:10.1161/01.CIR.0000070591.21548.69.

## Human Aortic Valve Calcification Is Associated With an Osteoblast Phenotype

**Nalini M. Rajamannan, MD, Malayannan Subramaniam, PhD, David Rickard, PhD, Stuart R. Stock, PhD, Janis Donovan, BS, Margaret Springett, Thomas Orszulak, MD, David A. Fullerton, MD, A.J. Tajik, MD, Robert O. Bonow, MD, and Thomas Spelsberg, PhD**

Divisions of Cardiology and Cardiothoracic Surgery (N.M.R., D.A.F., R.O.B.), Northwestern University Feinberg School of Medicine, and Institute for Bioengineering and Nanoscience in Advanced Medicine (S.R.S.), Northwestern University, Chicago, Ill, and Department of Molecular Biology and Biochemistry (M.S., D.R., T.S.), Department of Cardiology and Cardiothoracic Surgery (J.D., T.O., A.J.T.), and Electron Microscopy Laboratory (M.S.), Mayo Clinic, Rochester, Minn

### Abstract

**Background**—Calcific aortic stenosis is the third most common cardiovascular disease in the United States. We hypothesized that the mechanism for aortic valve calcification is similar to skeletal bone formation and that this process is mediated by an osteoblast-like phenotype.

**Methods and Results**—To test this hypothesis, we examined calcified human aortic valves replaced at surgery (n=22) and normal human valves (n=20) removed at time of cardiac transplantation. Contact microradiography and micro-computerized tomography were used to assess the 2-dimensional and 3-dimensional extent of mineralization. Mineralization borders were identified with von Kossa and Goldner's stains. Electron microscopy and energy-dispersive spectroscopy were performed for identification of bone ultrastructure and CaPO<sub>4</sub> composition. To analyze for the osteoblast and bone markers, reverse transcriptase–polymerase chain reaction was performed on calcified versus normal human valves for osteopontin, bone sialoprotein, osteocalcin, alkaline phosphatase, and the osteoblast-specific transcription factor Cbfa1. Microradiography and micro-computerized tomography confirmed the presence of calcification in the valve. Special stains for hydroxyapatite and CaPO<sub>4</sub> were positive in calcification margins. Electron microscopy identified mineralization, whereas energy-dispersive spectroscopy confirmed the presence of elemental CaPO<sub>4</sub>. Reverse transcriptase–polymerase chain reaction revealed increased mRNA levels of osteopontin, bone sialoprotein, osteocalcin, and Cbfa1 in the calcified valves. There was no change in alkaline phosphatase mRNA level but an increase in the protein expression in the diseased valves.

**Conclusions**—These findings support the concept that aortic valve calcification is not a random degenerative process but an active regulated process associated with an osteoblast-like phenotype.

### Keywords

valves; stenosis; calcium

---

After hypertension and coronary artery disease, aortic valve disease is the third most common cardiovascular disorder in the United States. This condition increases in prevalence

with advancing age, afflicting 4% of the population by age 80 years.<sup>1</sup> The natural history as described by Ross and Braunwald<sup>2</sup> indicates that severe symptomatic aortic stenosis is associated with a life expectancy of less than 5 years. Despite the high prevalence of this condition, little is known regarding the molecular basis of calcific aortic stenosis. Studies have determined that mature lamellar bone formation occurs in calcified human aortic valves and that these valves express osteopontin, a bone matrix protein important in the development of cardiovascular calcification.<sup>3,4</sup> Mohler et al<sup>5</sup> have also shown that human aortic valve cell cultures in vitro contain a calcifying cell possessing osteoblast-like features. In this study, we hypothesized that the extraosseous calcification in the human aortic valve resembles the regulated bone formation that occurs in the skeleton and involves the development of osteoblast-like features. We have recently demonstrated that a similar osteoblast phenotype develops in an experimental model of hypercholesterolemia-induced aortic valve disease.<sup>6</sup> We tested our hypothesis by examining human aortic valves for the expression of osteoblast markers as well as for the histological appearance of a mineralized bone-like matrix.

## Methods

### Human Calcified Aortic Valves

The use of all human tissue was approved by the Institutional Review Boards at the Mayo Clinic (1732-98) and Northwestern University (1041-001). We obtained human calcified valves from patients with aortic stenosis (n=22) at the time of surgical valve replacement and normal control valves at the time of heart transplantation (n=20). We also compared the calcified human aortic valves to control human femur and iliac bone from the Mayo Clinic Core Bone Laboratory, because the iliac bone is the standard control for the bone histomorphometric stains (bone controls not shown). On extraction, tissues were either immersed in formalin or fresh frozen and stored at -70.

### Detection of Bone-Like Matrix and Mineral in Aortic Valves

**Tissue Preparation**—The valve was infiltrated in the polymerize medium methyl methacrylate using controlled temperature embedding (Rainer Technical Products). Five-micron serial sections were cut for staining using a microtome with a D-profile knife (Leica).

**Contact Microradiography**—Contact microradiographs (150- to 200- $\mu$ m sections) were prepared by exposure of the 150- to 200- $\mu$ m sections to Kodak 1A High Resolution Photoplates (Microchrome Technology, Inc) using a Raymax 60 U with a continuously evacuated demountable tube and half-wave rectification. The unit was operated at 20 kV, and a copper target was chosen, because its characteristic radiation is absorbed selectively by hydroxyapatite, the bone mineral.<sup>7</sup>

**Staining**—The aortic valve and normal iliac bone biopsy were stained with Goldner's Modified Masson-Trichrome Stain,<sup>8</sup> staining hydroxyapatite green. The sections were stained with von Kossa to localize calcium phosphate crystals.

**Micro-Computerized Tomography**—Human aortic valve and human femur were examined using a Scanco MicroCT-40 system operated at 45 kV. Sampling was with  $\approx 8 \mu$ m voxels (volume elements), maximum sensitivity (1000 projections, 2048 samples, and 0.3 sec/projection integration). The specimen of human femur was used as a control for assessing the extent to which mineral levels in the valves approached those of the cortical bone. (Iliac controls are not shown.)

**Electron Microscopy and Energy-Dispersive Spectroscopy**—Histological samples were fixed as described previously.<sup>6</sup> Energy-dispersive spectroscopy was performed on a Phillips CM 12 electron microscope. Immunogold labeling for alkaline phosphatase (University of Iowa Hybridoma Bank) (1:10) was performed on normal versus calcified human aortic valves as described previously.<sup>6</sup>

### Reverse Transcriptase–Polymerase Chain Reaction

Total RNA extraction and reverse transcriptase–polymerase chain reaction (RT-PCR) analysis were performed for the expression of osteoblast marker genes, including osteopontin, bone sialoprotein, and osteocalcin, using the protocol and primer sequences described by Rickard et al,<sup>9</sup> with the exception of the primers for Cbfa-1, as described by Komori et al.<sup>10</sup>

## Results

### Establishment of the Bone-Like Phenotype in Calcified Human Aortic Valves

**Contact Microradiography and Staining**—We performed contact microradiography in conjunction with special bone histomorphometric staining to confirm the presence of calcification and mineralization in calcified valve tissues. The x-ray microradiograph in Figure 1A1 demonstrates areas of calcification within the valve leaflet. Figure 1A2 shows a high magnification and a low magnification of a serial section of the leaflet stained with Goldner's Modified Masson-Trichrome stain with an arrow pointing to the green staining hydroxyapatite synthesis. In Figure 1A3, the arrow in the high-magnification image of a section stained by von Kossa points to an area of black stain, indicating the presence of calcium phosphate crystals in the same areas of calcification shown in Figures 1A1 and 1A2.

**Micro-Computerized Tomography**—Two-dimensional (2D) and 3-dimensional (3D) analysis of the aortic valve by micro-computerized tomography (MicroCT) revealed the depth and extent of calcification in each nodule on the valve compared with a human femur bone. The section of the human femur was scanned to provide a reference for comparison with the mineralized valve (controls not shown). Figure 1B1 is a 2D graphic reconstruction of the calcified valve nodule, and Figure 1B2 is the 3D reconstruction. The 2D and 3D images indicate a pattern of mineralization that is heavier toward the outer edge of each nodule and diminished toward the center of the valve, and these were characteristic findings in all of the calcified valves. The x-ray of the human femur fragment and the mineralized valve were indistinguishable, except for the fine structure found in the center of the valve.

**Energy-Dispersive Spectroscopy**—The energy-dispersive spectroscopy scan indicates that the elemental composition of CaPO<sub>4</sub> in the areas of valve calcification is similar to that of normal skeletal bone, as shown in Figure 2A1.

**Reverse Transcriptase–Polymerase Chain Reaction**—To analyze the expression of osteoblast and bone matrix markers, mRNA was isolated from calcified and normal aortic valves, and RT-PCR was performed to compare the relative level of osteopontin, bone sialoprotein, osteocalcin, alkaline phosphatase, and the osteoblast-specific transcription factor Cbfa1. Figure 2A2 demonstrates that all markers were increased in the calcified aortic valves compared with the noncalcified controls, with the exception of alkaline phosphatase, which was unchanged.

**Electron Microscopy**—In the calcified aortic valves, heavily labeled patches of alkaline phosphatase were concentrated over cells (Figure 2B1) and dense extracellular matrix. In the normal aortic valves, a few nonspecific gold particles were scattered over the

heterochromatin of fibroblasts (control aortic valves not shown). In Figure 2B2, the ultrastructure of calcified human aortic valve shows collagen bundles interspersed with multiple focal electron-dense deposits that have been identified as hydroxyapatite by EDS analysis.

## Discussion

In this study, we demonstrate that calcification in human aortic valve leaflets has similar features to that of osteoblastogenesis during skeletal bone formation. Bone is a mineralized connective tissue, comprising an exquisite assembly of functionally distinct cell populations that are required to support the structural integrity of the skeleton. The *ex vivo* demonstration of mineralization areas in the calcified aortic valve using microCT in this study may relate to the clinical use of electron beam computed tomography to study the *in vivo* progression of aortic valve calcification.<sup>11</sup>

Skeletal bone formation requires that osteoblast cells derived from mesenchymal precursor cells in the bone marrow stroma and periosteum differentiate into osteoblasts capable of depositing a mineralized extracellular matrix.<sup>12</sup> Genes characteristic of osteoblastic cells include those encoding for alkaline phosphatase, osteopontin, osteocalcin, and bone sialoprotein.<sup>13</sup> These markers are mostly bone extracellular matrix molecules and late markers of osteoblast differentiation expressed during active mineralization. Two important osteoblast-specific transcripts have been identified, those encoding *Cbfa1* and osteocalcin.<sup>14</sup> During embryonic development, *Cbfa1* expression precedes osteoblast differentiation and is restricted to mesenchymal cells destined to become osteoblasts.<sup>14</sup> Thus, the expression of *Cbfa1* may play a role in valvular calcification. Osteocalcin is a late marker of calcification in osteoblastogenesis and is present in the later stages of skeletal bone formation.<sup>12</sup> In the vasculature, Watson et al<sup>15</sup> have demonstrated that an osteoblast-like vascular cell resides in the medial layer of the vascular aorta, which may contribute to arterial calcification. In this study, we have demonstrated increased mRNA levels for several markers important in bone formation in the diseased human aortic valves except alkaline phosphatase. However, immunogold labeling for protein expression of alkaline phosphatase was increased and localized to areas of calcified extracellular matrix in the calcified valve.

Our new observations in human aortic valves, together with data from our *in vivo* animal model of aortic valve disease and other *in vitro* vascular calcification models,<sup>6,15</sup> support the hypothesis that degenerative valvular aortic stenosis is the result of active bone formation in the aortic valve, which may be mediated through a process of osteoblast-like differentiation in these tissues.

## References

1. Lindroos M, Kupari M, Heikkilä J, et al. Prevalence of aortic valve abnormalities in the elderly: an echocardiographic study of a random population sample. *J Am Coll Cardiol.* 1993; 21:1220–1225. [PubMed: 8459080]
2. Ross J, Braunwald E. Aortic stenosis. *Circulation.* 1968; 381(suppl):61–67. [PubMed: 4894151]
3. Mohler ER, Gannon F, Reynolds C, et al. Bone formation and inflammation in cardiac valves. *Circulation.* 2001; 103:1522–1528. [PubMed: 11257079]
4. O'Brien KD, Kuusisto J, Reichenbach DD, et al. Osteopontin is expressed in human aortic valvular lesions. *Circulation.* 1995; 92:2163–2168. [PubMed: 7554197]
5. Mohler ER, Chawla MK, Chang AW, et al. Identification and characterization of calcifying valve cells from human and canine aortic valves. *J Heart Valve Dis.* 1999; 8:254–260. [PubMed: 10399657]

6. Rajamannan NM, Subramaniam M, Springett M, et al. Atorvastatin inhibits hypercholesterolemia-induced cellular proliferation and bone matrix production in the rabbit aortic valve. *Circulation*. 2002; 105:2660–2665. [PubMed: 12045173]
7. Jowsey J. Age changes in human bone. *Clin Orthop*. 1960; 17:210–218.
8. *Tissue and Special Stains Catalog*. Rochester, Minn: Mayo Medical Laboratories, Mayo Clinic and Mayo Foundation; 1993.
9. Rickard DJ, Kassem M, Hefferan T, et al. Isolation and characterization of osteoblast precursor cells from human bone marrow. *J Bone Miner Res*. 1996; 11:312–324. [PubMed: 8852942]
10. Komori T, Yagi H, Nomura S, et al. Targeted disruption of *Cbfa1* results in a complete lack of bone formation owing to maturational arrest of osteoblasts. *Cell*. 1997; 89:755–784. [PubMed: 9182763]
11. Shavelle DM, Takasu J, Budoff MJ, et al. HMG CoA reductase inhibitor (statin) and aortic valve calcium. *Lancet*. 2002; 359:1125–1126. [PubMed: 11943265]
12. Gehron Robey, P.; Boskey, AL. The biochemistry of bone. In: Marcus, R.; Feldman, D., editors. *Osteoporosis*. New York: Raven Press; 1996. p. 95-184.
13. Aubin JE, Liu F, Malaval L, et al. Osteoblast and chondroblast differentiation. *Bone*. 1995; 17:77S–83S. [PubMed: 8579903]
14. Karsenty G, Ducy P, Starbuck M, et al. *Cbfa1* as a regulator of osteoblast differentiation and function. *Bone*. 1999; 25:107–108. [PubMed: 10423032]
15. Watson KE, Bostrom K, Ravindranath R, et al. TGF-beta 1 and 25-hydroxycholesterol stimulate osteoblast-like vascular cell to calcify. *J Clin Invest*. 1994; 93:2106–2013.

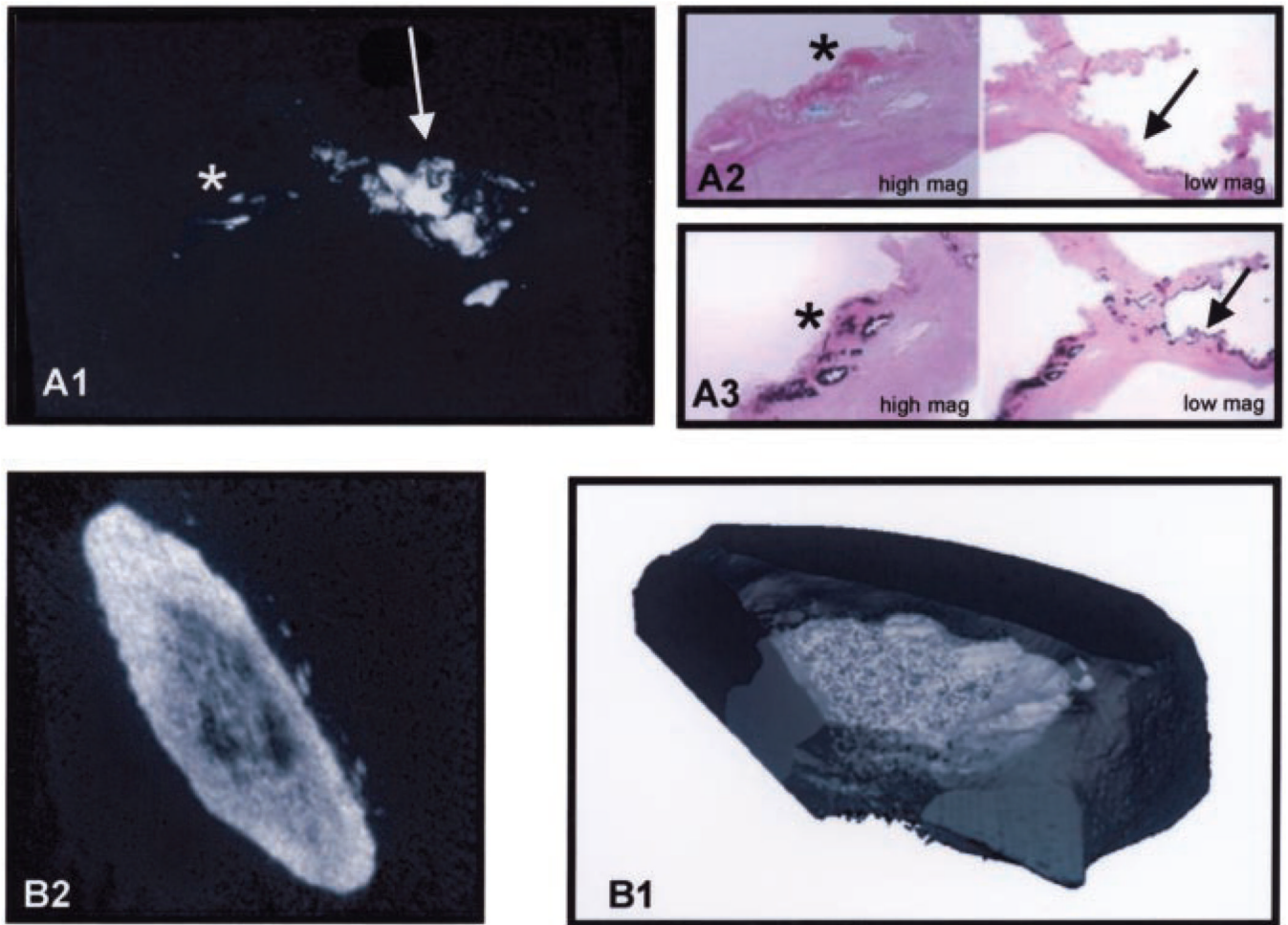


**Figure 1.** Histomorphometry of the calcified aortic valve. A1, X-ray microradiograph of the calcified valve. The smaller area of calcification is on the right, denoted by a star, and an arrow is pointing to the larger area of calcification on the left. A2, Star points to the Goldner's-Masson Trichrome green stain for hydroxyapatite in the low magnification view. A3, Arrow points to the von Kossa black stain for calcium and phosphate in the high-magnification view. B1, MicroCT 2D reconstruction of the calcified aortic valve. B2, MicroCT 3D reconstruction of the calcified aortic valve.

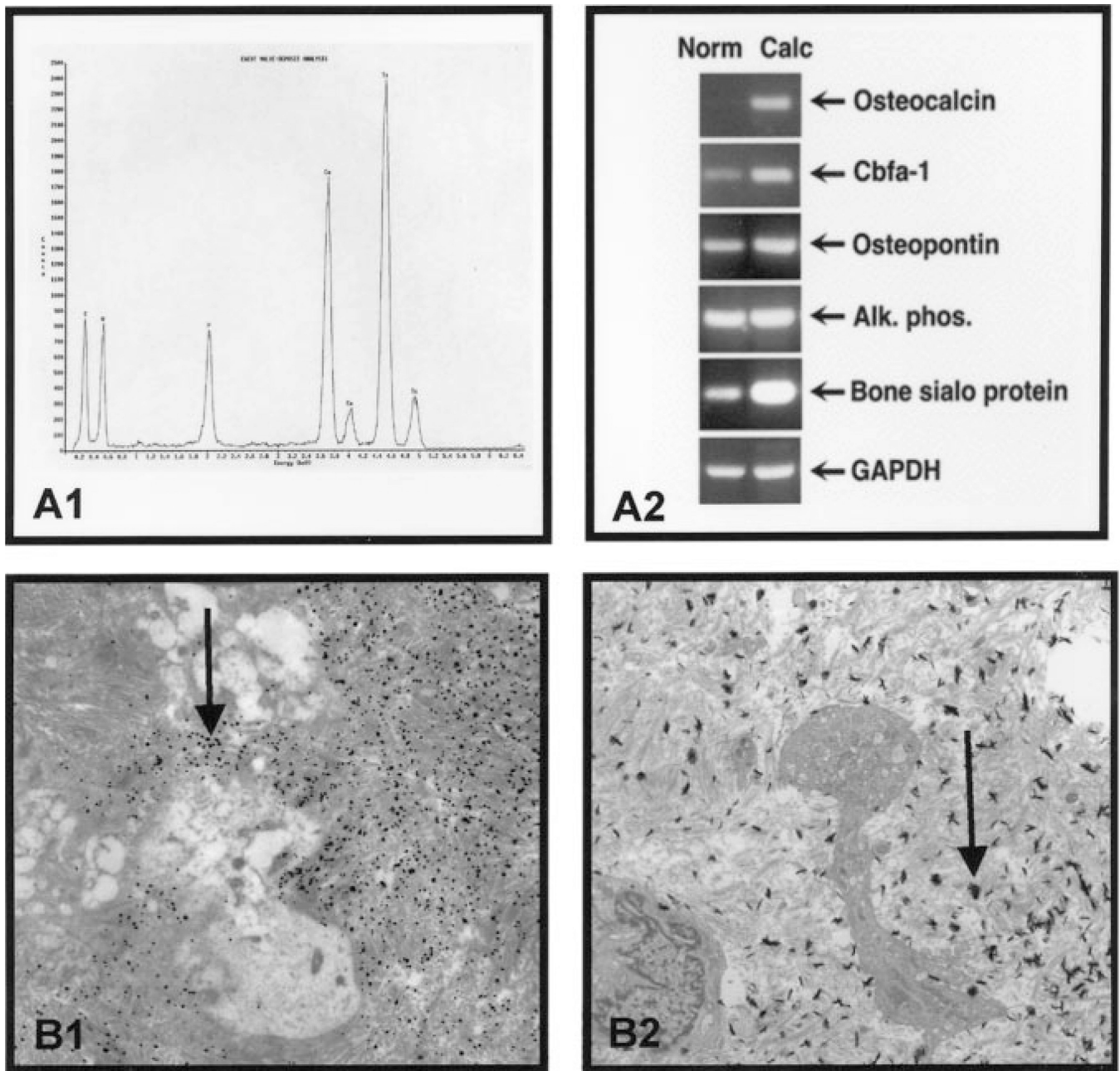


**Figure 2.** Phenotype of the calcified aortic valve. A1, Electron dispersive spectroscopy confirms the presence of elemental  $\text{CaPO}_4$ . A2, Semi-quantitative RT-PCR. RT-PCR using the total RNA for the bone markers demonstrating an increase in the RNA expression in all markers except alkaline phosphatase. B1, Immunogold electron microscopy. The arrow points to the alkaline phosphatase gold label in the calcified aortic valves, demonstrating a marked increase in label. B2, Electron microscopy. The arrow points to an area of mineralization in the valve (34K).